α,ω-dihexyl-sexithiophene thin films for solution-gated organic field-effect transistors

Hannah Schamoni,[1] Simon Noever,[2] Bert Nickel,[2] Martin Stutzmann,[1] and Jose A. Garrido[3,4,a)]
[1]*Walter Schottky Institut and Physik-Department, Technische Universität München, Am Coulombwall 4, 85748 Garching, Germany*
[2]*Fakultät für Physik und CeNS, Ludwig-Maximilians-Universität München, Geschwister-Scholl-Platz 1, 80539 München, Germany*
[3]*Catalan Institute of Nanoscience and Nanotechnology (ICN2), CSIC and The Barcelona Institute of Science and Technology, Campus UAB, Bellaterra, 08193 Barcelona, Spain*
[4]*ICREA, Institució Catalana de Recerca i Estudis Avantçats, 08070 Barcelona, Spain*

(Received 30 July 2015; accepted 8 February 2016; published online 19 February 2016)

While organic semiconductors are being widely investigated for chemical and biochemical sensing applications, major drawbacks such as the poor device stability and low charge carrier mobility in aqueous electrolytes have not yet been solved to complete satisfaction. In this work, solution-gated organic field-effect transistors (SGOFETs) based on the molecule α,ω-dihexyl-sexithiophene (DH6T) are presented as promising platforms for in-electrolyte sensing. Thin films of DH6T were investigated with regard to the influence of the substrate temperature during deposition on the grain size and structural order. The performance of SGOFETs can be improved by choosing suitable growth parameters that lead to a two-dimensional film morphology and a high degree of structural order. Furthermore, the capability of the SGOFETs to detect changes in the *p*H or ionic strength of the gate electrolyte is demonstrated and simulated. Finally, excellent transistor stability is confirmed by continuously operating the device over a period of several days, which is a consequence of the low threshold voltage of DH6T-based SGOFETs. Altogether, our results demonstrate the feasibility of high performance and highly stable organic semiconductor devices for chemical or biochemical applications. © *2016 AIP Publishing LLC*. [http://dx.doi.org/10.1063/1.4942407]

Organic semiconductors offer the possibility to fabricate devices featuring biocompatibility,[1,2] mechanical flexibility,[3–5] and comparably low production costs.[1,2] Therefore, a wide range of applications employing organic semiconductors is being currently explored in the fields of biosensing and biomedical technologies.[6–8] Among other molecules, oligothiophenes have been studied intensively for their suitability to be applied in field-effect transistors.[9–17] In the case of solution-gated organic field-effect transistors (SGOFETs), the organic semiconductor is gated through an electrolyte. An electrical double layer, characterized by a rather high interfacial capacitance, builds up at the semiconductor-liquid interface. Consequently, the applied gate bias voltage may be kept well under 1 V,[18–20] leading to an improved device stability and the possibility of in-electrolyte applications.[8,16,17,21,22] Using α-sexithiophene (6T) as active material, biofunctional sensors for the detection of penicillin have been demonstrated previously.[17] However, the stability of the device strongly depends on the characteristics of the employed organic molecules. It is, therefore, of utmost importance to explore the use of molecules which could eventually lead to an improved device stability.

In this work, we report on the implementation of the end-substituted molecule α,ω-dihexyl-sexithiophene (DH6T) in SGOFETs. DH6T has been reported to exhibit favorable properties like an improved structural order in thin films and an increased field-effect mobility as compared to the unsubstituted 6T.[23,24] Here, we demonstrate the influence of the substrate temperature during deposition on the morphology and structural order of the thin film by atomic force microscopy (AFM), X-ray reflectivity (XRR), and UV-Vis spectroscopy. Furthermore, we characterize SGOFETs based on DH6T with regard to transistor performance and stability, and we reveal their sensitivity towards changes in the *p*H and ionic strength of the gate electrolyte.

Organic thin films of DH6T (nominal thickness: 30 nm) were deposited on sapphire substrates by organic molecular beam deposition in an ultrahigh vacuum system as described previously.[16,17] In order to tune the morphology of the deposited films, the temperature of the sapphire substrate T_{sub} during thin film deposition was varied between room temperature (19 °C) and 55 °C. Typical deposition rates are between 0.5 and 2 Å/min. The fabrication details of the SGOFETs (width-to length ratio of the transistor channel: $W/L = 4900$) have been described elsewhere[16,17] and remained unchanged in this work, except for the contact thickness (5 nm Ti/45 nm Au). All measurements were carried out in ambient atmosphere. The transistor and stability characterization and the ion sensing experiments were performed in a 5 mM phosphate buffered saline (PBS) solution at *p*H 5. To change the ionic strength, KCl solution was added to the buffer. For the *p*H sensing measurements, a 10 mM PBS solution, whose ionic strength was adjusted to 50 mM with KCl (KPBS), was used. The *p*H was altered by adding either HCl or KOH solution. The gate voltage was applied via an Ag/AgCl reference electrode in all cases.

a)Author to whom correspondence should be addressed. Electronic mail: joseantonio.garrido@icn.cat

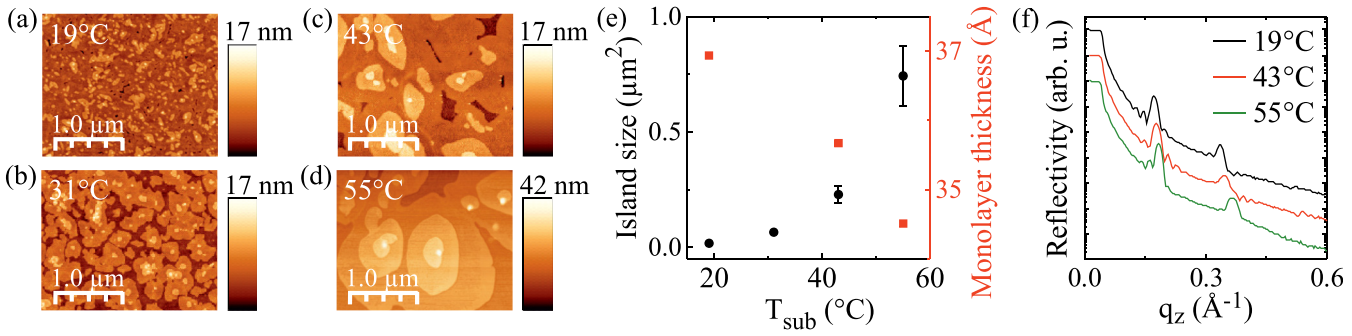

FIG. 1. Characterization of nominally 30 nm thick DH6T thin films deposited at different substrate temperatures. (a) AFM micrographs for $T_{sub} = 19\,^{\circ}\mathrm{C}$ (room temperature), (b) $T_{sub} = 31\,^{\circ}\mathrm{C}$, (c) $T_{sub} = 43\,^{\circ}\mathrm{C}$, and (d) $T_{sub} = 55\,^{\circ}\mathrm{C}$. (e) Average size of the grains versus T_{sub} as extracted from AFM images (black dots) and monolayer thickness in the thin films (red squares) as a function of T_{sub}. The latter was calculated from the position of the first order peak in the X-ray reflectivity spectra of the deposited DH6T films (f).

The temperature of the sapphire substrate T_{sub} was varied and its influence on the morphology of the DH6T layers was investigated. As the AFM micrographs in Figures 1(a)–1(d) illustrate, the grains are larger and exhibit a more three-dimensional topography for higher temperatures. This is understood in terms of an extended diffusion length of molecules with rising temperatures on the substrate surface.[25] A quantitative analysis of the average island size for different values of T_{sub} is shown in Figure 1(e) (black dots).

To investigate possible changes in the thin film structure itself, XRR spectra were recorded for films deposited at different T_{sub} (see Figure 1(f)). Garnier *et al.* have reported a monoclinic unit cell in DH6T thin films with an angle $\beta = 111.3^{\circ}$ and a tilt angle between core and side chains of 16°, leading to an effective molecule length of 38.1 Å.[23] The theoretical value of the monolayer thickness thereby calculates to 35.5 Å. From the position of the first order peak, q_1, the monolayer thickness d of the investigated thin films can be calculated via $d = 2\pi/q_1$. As illustrated in Figure 1(e) (red squares), it lies in the expected range; however, a decrease in the monolayer thickness with increasing T_{sub} is observed, which may be due to a change in the tilt angle of the DH6T molecules towards the substrate surface normal. In addition, the first order peak in the XRR spectra becomes more intense with increasing substrate temperature (see Figures S1(a) and S1(b) (Ref. 26)), indicating a higher degree of structural order in these thin films, as discussed in the following.

Additional information related to the structural order can be obtained from UV-Vis spectroscopy. Absorption spectra of DH6T thin films deposited at various T_{sub} are depicted in Figure 2(a). These are normalized to the intensity of the most prominent peak at about 3.3 eV, which corresponds to the HOMO → LUMO transition of molecules for which the interaction with neighboring molecules leads to a Davydov splitting of the LUMO.[27,28] This absorption peak is most intense and narrow, if the transition dipoles of all molecules are aligned in parallel. The normalized spectra illustrate a change in the shape of this peak with T_{sub}, suggesting a change in the interaction between molecules in the thin film. The quantitative analyses of the average peak intensity and full width at half maximum (FWHM) (Figure 2(b)) reveal an increase in the peak intensity and a decrease in the FWHM with increasing T_{sub} (see Figure S2(a) for non-normalized spectra[26]). These findings indicate an increase in the degree of structural order of the thin films for higher substrate temperatures, in agreement with the XRR data presented above. In contrast, no dependence on T_{sub} was found for the intensity of the peak at 4.3 eV (see Figure S2(b) (Ref. 26)). Such a peak has already been observed for thin films of oligothiophenes of various conjugation core lengths and with different substituents and is attributed to the absorption of a single thiophene unit.[29] Its independence of T_{sub} originates from the molecular character of the corresponding transition, as opposed to the crystalline HOMO → LUMO transition located at 3.3 eV.

DH6T thin films were used as the active material in SGOFETs, the layout of which is sketched in Figure 3(a). The Ti/Au contact pattern was predefined by photolithography, deposited via thermal evaporation and partly covered by a photoresist prior to the organic thin film growth. Exemplary transistor output curves in a 5 mM PBS buffer at *p*H 5 are shown in Figure 3(b). They show a current level of several 10 µA and saturation behavior for high drain-source voltages. Furthermore, the gate-source current is three orders of magnitude smaller than I_{DS}, and cyclic voltammetry measurements show no indication of Faradaic processes in the potential window of the SGOFETs (see Figures S3(a) and 3(b) (Ref. 26)). Therefore, we can conclude that the current modulation is dominated by the field-effect, in agreement with previous reports.[20,30] From the transfer curve at a drain-source voltage $U_{DS} = -50\,\mathrm{mV}$ (black dots in Figure 3(c)), a

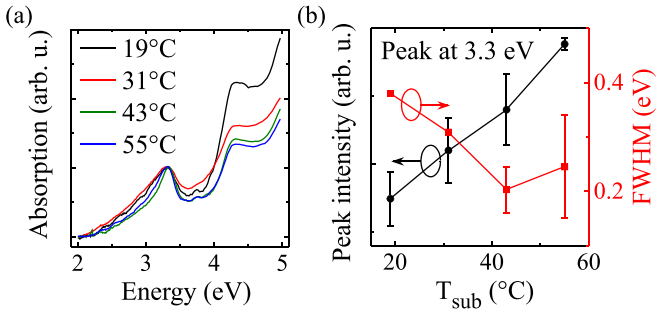

FIG. 2. Optical characterization by UV-Vis spectroscopy of 30 nm thick DH6T films deposited at different substrate temperatures. (a) Absorption spectra, normalized by the intensity of the peak at 3.3 eV. (b) Average intensity (black dots) and FWHM (red squares) of the same peak as a function of T_{sub}. The lines were added as a visual guidance. The error bars represent the standard error of the mean values.

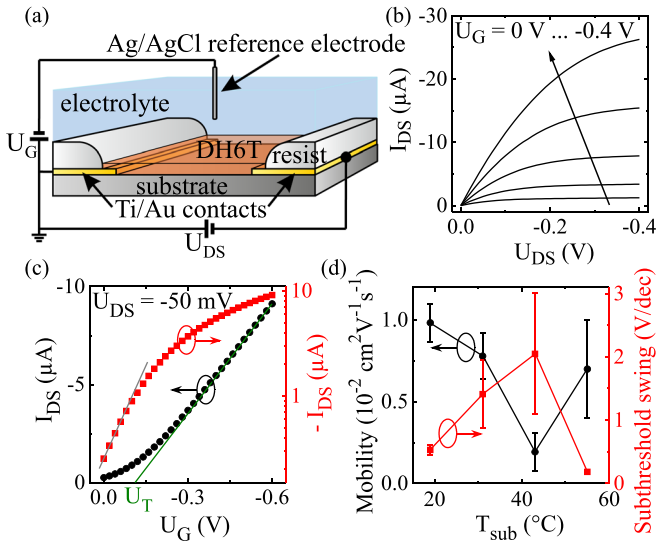

FIG. 3. Electrical characterization of SGOFETs using 30 nm thick films of DH6T as the active material. The measurements were conducted in 5 mM PBS at *p*H 5. (a) Device layout. The width-to-length ratio is 4900. (b) Typical output characteristics and (c) corresponding transfer curve at $U_{DS} = -50$ mV on a linear (black dots) and logarithmic scale (red squares). Linear fits to the data are represented by the solid lines and the threshold voltage U_T is indicated. The DH6T thin film of this sample was deposited at $T_{sub} = 19\,°C$. (d) Field-effect mobility (black dots) and subthreshold swing (red squares) versus T_{sub} as extracted from the transfer curves. The lines were added as a visual guidance. The error bars represent the standard error of the mean values (see supplementary material[26]).

transconductance $g_m = 18\,\mu S$ was obtained, which can be used to determine the field-effect mobility μ via $\mu = g_m/(C_{dl}U_{DS})\,L/W$. In this equation, C_{dl} is the electrical double layer capacitance of the semiconductor-electrolyte interface, which was estimated to 4 μF/cm^2 via electrochemical impedance spectroscopy (see Figure S4 (Ref. 26)). This compares well to the interfacial capacitances of other solution-gated organic field effect transistor systems.[16,31,32] From the maximum transconductance of the devices, we can estimate a field-effect mobility of up to about 1×10^{-2} cm^2/V s for the discussed set of transistors (Figure 3(d)) and of up to 1.9×10^{-2} cm^2/V s for devices which organic thin film was deposited at different rates. It is worth noting that the threshold voltage U_T of about -0.1 V is significantly lower than what has been reported for 6T-based SGOFETs of the same layout ($U_T \lesssim -0.3$ V).[16,17] Such a low U_T might be due to favorable values of, for example, C_{dl}, the surface charge of the semiconductor or the work function of the DH6T molecules.[33] Above all, it enables the operation of the SGOFETs at low voltages, which is of utmost importance for a good device stability.[8,16,17] To additionally characterize the current onset of the transistors, the subthreshold swing was extracted from a logarithmic plot of the transfer curve (red squares in Figure 3(c)). Its theoretical limit at room temperature is 60 mV/dec.[34] Values as low as 160 mV/dec confirm a fast switching behavior of our devices. The deviation from the theoretical limit may result from defect states at the semiconductor-electrolyte interface or from the chosen device geometry.[34]

Furthermore, the influence of the morphology of the thin films on the transistor characteristics was studied by evaluating field-effect mobility and subthreshold swing as a function of the substrate temperature during deposition. Figure 3(d) (black dots) illustrates that the best performance was observed at the lowest and highest temperature. This possibly indicates two competing effects: On the one hand, the films are more two-dimensional at low T_{sub} (cf. Figures 1(a)–1(e)), which enhances charge transport and, thus, the field-effect mobility.[35] On the other hand, the analysis of the structural properties suggests an improved degree of ordering at high T_{sub}. An increase in structural order has also been reported for α,ω-DH6T thin films in comparison to films of β,β'-DH6T or unsubstituted 6T, and it has been correlated to an increase in field-effect mobility.[23] Thus, the anew increase in mobility at high T_{sub} may presumably be attributed to an improvement of the structural order in the film. As Figure 3(d) (red squares) further illustrates, the subthreshold swing confirms this interpretation: a faster on-switching of the SGOFETs (low subthreshold swing values) is enabled by a two-dimensional film morphology (lowest T_{sub}) and a high degree of structural order (highest T_{sub}). Nevertheless, it has to be noted that the effect of T_{sub} on the thin film is more pronounced for the increase from room temperature to 43 °C than for the change from 43 °C to 55 °C (cf. Figures 1(a)–1(d)). More data statistics will be needed in order to verify the observed trend in μ and in the subthreshold swing (cf. Figure 3(d); see Figure S5 for a visualization of the statistics of μ used in this work[26]). From the correlation of the subthreshold swing with both the defect density and the field-effect mobility, it may also be concluded that the good transistor performance is the result of a low defect density.

The capability of the DH6T-based SGOFETs to be applied as sensors in aqueous electrolytes, in this particular case as *p*H sensors, is demonstrated in Figure 4(a). With decreasing *p*H of the buffer solution, the transfer curves shift to more negative gate voltages, while g_m stays unchanged. Therefore, the *p*H sensitivity is given by the change in gate voltage U_G per *p*H with respect to U_G at neutral *p*H for a fixed value of the drain-source current I_{DS}. U_G experiences a linear dependence over a wide *p*H range without any hysteresis between decreasing and increasing *p*H, yielding a sensitivity of 14 mV/*p*H. According to the amphifunctional model, which is described in detail in the supplementary material,[26] the response of the transistor originates from a *p*H-dependent surface charge σ_{surf} at the semiconductor-electrolyte interface.[36] In order to obtain a good match between experimental data and a simulation using the amphifunctional model (blue line in Figure 4(b)), a monolayer coverage with hydroxide ions and an ionizable surface group of pK_a 3.3 have to be assumed. The latter group can be ascribed to oxygen-related moieties.[17] These findings are in agreement with those by Buth *et al.* for devices using 6T as organic semiconductor.[17]

Besides the study of the *p*H sensitivity, the sensitivity of the devices to changes in the ionic strength was investigated by adding KCl to the solution. In Figure 4(c), the corresponding change in U_G for a fixed value of I_{DS} is plotted logarithmically versus the salt activity for two different *p*H values of the buffer. The ion sensitivity is defined as the slope of the linear fit to the curves at high activity ($a \gtrsim 50$ mmol/kg), yielding values of -42 mV/dec at *p*H 5 and -30 mV/dec at *p*H 3 for the presented SGOFET. The ion sensitivity has been

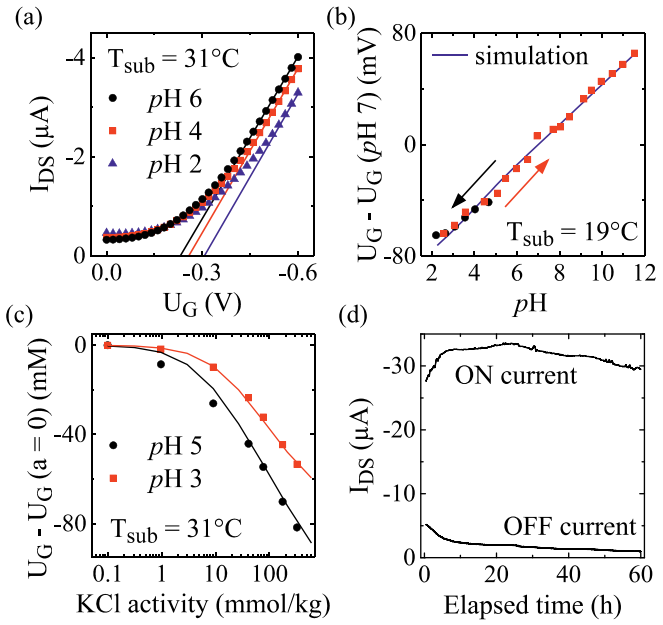

FIG. 4. Sensing and stability properties of SGOFETs. (a) Transfer curves recorded at three different *p*H values of the KPBS buffer. The solid lines represent fits to the linear regions. (b) Shift of U_G as a function of the *p*H of the electrolyte, together with a simulation of the data using the amphifunctional model. (c) Shift of U_G (compared to U_G at a salt activity $a = 0$ mM) as a function of the activity of KCl in the PBS buffer, which *p*H was adjusted to two different values. The solid lines represent simulations of the experimental data using the amphifunctional model. The substrate temperatures at which the DH6T thin films used in (a)–(c) were deposited are indicated in the graphs. (d) Evolution of the drain-source current I_{DS} during continuous cycling of U_G between 0 V and − 0.6 V for $U_{DS} = -0.2$ V, measured in 5 mM PBS at *p*H 5 and in the dark (deposition temperature of the DH6T thin film: $T_{sub} = 31$ °C). For clarity, only the maxima (ON current) and minima (OFF current) of the measured curve are shown in the graph.

interpreted in terms of the screening of the surface charge due to an increase in the diffuse charge.[37] If the surface charge is more negative, i.e., if the buffer is less acidic, the ion screening is more effective, which is confirmed by the higher sensitivity at *p*H 5 as compared to *p*H 3. Using a model similar to the amphifunctional model introduced by Härtl *et al.*,[37] the experimental data could be reproduced (solid lines in Figure 4(c)) assuming surface charges of $-5.6\,\mu C/cm^2$ at *p*H 5 and $-3.5\,\mu C/cm^2$ at *p*H 3, respectively, in agreement with the calculations by Buth *et al.* for 6T-SGOFETs.[16]

For applications of organic SGOFETs, the device stability during operation is of vital importance. A stability test was performed by switching on and off the SGOFETs continuously. To this end, the gate voltage was cycled between 0 V and −0.6 V for approximately 60 h, while applying a constant drain-source voltage of −0.2 V and recording the drain-source current. Here, the high current level decreased by only 10% with respect to the value after the initial increase in on-current (Figure 4(d)). The latter has been reported before by Roberts *et al.* for organic field-effect transistors immersed into an aqueous environment.[38,39] However, in contrast to the work by Roberts *et al.*, we observed a slight decrease in the off-current over time (see Figure 4(d)). As the transconductance of the respective device increased from 13 μS to 16 μS throughout the measurement and the subthreshold swing was reduced from about 550 mV/dec to 230 mV/dec, both changes may possibly be attributed to the passivation of trap states at the semiconductor-electrolyte interface by water molecules penetrating into the thin film.[34]

In summary, vacuum-evaporated thin films of the organic semiconductor DH6T were investigated by AFM, XRR, and UV-Vis spectroscopy. We could show that with increasing substrate temperature, the films exhibit an increasingly three-dimensional topography and feature a higher degree of structural order. At the same time, the tilt angle of the molecules towards the substrate surface normal appears to increase. Furthermore, we have fabricated and characterized SGOFETs using these thin films as the active material. The obtained characteristics are comparable to or even exceed those of analogous devices based on 6T.[16,17] In particular, the low threshold voltage is beneficial for a good transistor stability. Field-effect mobility and subthreshold swing were found to be correlated to the morphology and structural order of the films. This implies that the transistor performance can, to some extent, be tuned by the substrate temperature. Additionally, both *p*H and ion sensitivity of the SGOFETs were demonstrated, and the data could be simulated using suitable modifications of the amphifunctional model.[16,17,36,37] Finally, a good device stability was confirmed by switching it on and off continuously over a period of 60 h. The initial increase in the on-off ratio was tentatively attributed to the passivation of trap states at the semiconductor-electrolyte interface by water molecules. During the period of 60 h, the current level decreased by only 10%. In conclusion, SGOFETs based on DH6T are promising platforms for stable in-electrolyte sensing applications. By carefully choosing the growth parameters of the organic thin film, the performance may possibly be further improved.

This work has been partially supported by the Nanosystems Initiative Munich (NIM) and the Deutsche Forschungsgemeinschaft (DFG) through the SFB 1032.

[1]M. Irimia-Vladu, P. A. Troshin, M. Reisinger, L. Shmygleva, Y. Kanbur, G. Schwabegger, M. Bodea, R. Schwdiauer, A. Mumyatov, J. W. Fergus, V. F. Razumov, H. Sitter, N. S. Sariciftci, and S. Bauer, Adv. Funct. Mater. **20**, 4069 (2010).
[2]G. Scarpa, A.-L. Idzko, S. Götz, and S. Thalhammer, Macromol. Biosci. **10**, 378 (2010).
[3]T. Someya, T. Sekitani, S. Iba, Y. Kato, H. Kawaguchi, and T. Sakurai, Proc. Natl. Acad. Sci. **101**, 9966 (2004).
[4]S. Richter, M. Ploetner, W.-J. Fischer, M. Schneider, P.-T. Nguyen, W. Plieth, N. Kiriy, and H.-J. Adler, Thin Solid Films **477**, 140 (2005).
[5]D. Feili, M. Schuettler, T. Doerge, S. Kammer, K. P. Hoffmann, and T. Stieglitz, J. Micromech. Microeng. **16**, 1555 (2006).
[6]C. Bartic, B. Palan, A. Campitelli, and G. Borghs, Sens. Actuators, B **83**, 115 (2002).
[7]T. Someya, A. Dodabalapur, J. Huang, K. C. See, and H. E. Katz, Adv. Mater. **22**, 3799 (2010).
[8]L. Kergoat, B. Piro, M. Berggren, M.-C. Pham, A. Yassar, and G. Horowitz, Org. Electron. **13**, 1 (2012).
[9]A. Tsumura, H. Koezuka, and T. Ando, Appl. Phys. Lett. **49**, 1210 (1986).
[10]H. Akimichi, K. Waragai, S. Hotta, H. Kano, and H. Sakaki, Appl. Phys. Lett. **58**, 1500 (1991).
[11]Z. Bao, A. Dodabalapur, and A. J. Lovinger, Appl. Phys. Lett. **69**, 4108 (1996).
[12]R. Hajlaoui, D. Fichou, G. Horowitz, B. Nessakh, M. Constant, and F. Garnier, Adv. Mater. **9**, 557 (1997).
[13]C. D. Dimitrakopoulos, B. K. Furman, T. Graham, S. Hegde, and S. Purushothaman, Synth. Met. **92**, 47 (1998).

[14]M. Halik, H. Klauk, U. Zschieschang, G. Schmid, S. Ponomarenko, S. Kirchmeyer, and W. Weber, Adv. Mater. **15**, 917 (2003).
[15]A. Facchetti, M. Mushrush, M-H. Yoon, G. R. Hutchison, M. A. Ratner, and T. J. Marks, J. Am. Chem. Soc. **126**, 13859 (2004).
[16]F. Buth, D. Kumar, M. Stutzmann, and J. A. Garrido, Appl. Phys. Lett. **98**, 153302 (2011).
[17]F. Buth, A. Donner, M. Sachsenhauser, M. Stutzmann, and J. A. Garrido, Adv. Mater. **24**, 4511 (2012).
[18]M. J. Panzer, C. R. Newman, and C. D. Frisbie, Appl. Phys. Lett. **86**, 103503 (2005).
[19]L. Herlogsson, X. Crispin, N. D. Robinson, M. Sandberg, O.-J. Hagel, G. Gustafsson, and M. Berggren, Adv. Mater. **19**, 97 (2007).
[20]M. J. Panzer and C. D. Frisbie, J. Am. Chem. Soc. **129**, 6599 (2007).
[21]B. Baur, J. Howgate, H.-G. von Ribbeck, Y. Gawlina, V. Bandalo, G. Steinhoff, M. Stutzmann, and M. Eickhoff, Appl. Phys. Lett. **89**, 183901 (2006).
[22]H. U. Khan, J. Jang, J.-J. Kim, and W. Knoll, J. Am. Chem. Soc. **133**, 2170 (2011).
[23]F. Garnier, A. Yassar, R. Hajlaoui, G. Horowitz, F. Deloffre, B. Servet, S. Ries, and P. Alnot, J. Am. Chem. Soc. **115**, 8716 (1993).
[24]B. Servet, G. Horowitz, S. Ries, O. Lagorsse, P. Alnot, A. Yassar, F. Deloffre, P. Srivastava, and R. Hajlaoui, Chem. Mater. **6**, 1809 (1994).
[25]R. Ruiz, D. Choudhary, B. Nickel, T. Toccoli, K.-C. Chang, A. C. Mayer, P. Clancy, J. M. Blakely, R. L. Headrick, S. Iannotta, and G. G. Malliaras, Chem. Mater. **16**, 4497 (2004).
[26]See supplementary material at http://dx.doi.org/10.1063/1.4942407 for an evaluation of the peak intensity in the XRR spectra, non-normalized UV-Vis spectra, gate-source current and cyclic voltammetry data, electrochemical impedance spectroscopy data, the statistics of the field-effect mobility data, and a detailed description of the amphifunctional model.
[27]A. Yassar, G. Horowitz, P. Valat, V. Wintgens, M. Hmyene, F. Deloffre, P. Srivastava, P. Lang, and F. Garnier, J. Phys. Chem. **99**, 9155 (1995).
[28]M. Muccini, E. Lunedei, C. Taliani, D. Beljonne, J. Cornil, and J. L. Brédas, J. Chem. Phys. **109**, 10513 (1998).
[29]A. Facchetti, M.-H. Yoon, C. L. Stern, G. R. Hutchison, M. A. Ratner, and T. J. Marks, J. Am. Chem. Soc. **126**, 13480 (2004).
[30]G. Tarabella, C. Santato, S. Y. Yang, S. Iannotta, G. G. Malliaras, and F. Cicoira, Appl. Phys. Lett. **97**, 123304 (2010).
[31]L. Kergoat, L. Herlogsson, D. Braga, B. Piro, M.-C. Pham, X. Crispin, M. Berggren, and G. Horowitz, Adv. Mater. **22**, 2565 (2010).
[32]L. H. Hess, M. V. Hauf, M. Seifert, F. Speck, T. Seyller, M. Stutzmann, I. D. Sharp, and J. A. Garrido, Appl. Phys. Lett. **99**, 033503 (2011).
[33]R. Schroeder, L. A. Majewski, and M. Grell, Appl. Phys. Lett. **83**, 3201 (2003).
[34]S. M. Sze and K. K. Ng, *Physics of Semiconductor Devices*, 3rd ed. (Wiley-Interscience, Hoboken and N.J, 2007).
[35]J. Locklin, M. E. Roberts, S. C. B. Mannsfeld, and Z. Bao, J. Macromol. Sci., Part C: Polym. Rev. **46**, 79 (2006).
[36]J. Duval, J. Lyklema, J. M. Kleijn, and H. P. van Leeuwen, Langmuir **17**, 7573 (2001).
[37]A. Härtl, J. A. Garrido, S. Nowy, R. Zimmermann, C. Werner, D. Horinek, R. Netz, and M. Stutzmann, J. Am. Chem. Soc. **129**, 1287 (2007).
[38]M. E. Roberts, S. C. B. Mannsfeld, N. Queralto, C. Reese, J. Locklin, W. Knoll, and Z. Bao, Proc. Natl. Acad. Sci. **105**, 12134 (2008).
[39]M. E. Roberts, S. C. B. Mannsfeld, M. L. Tang, and Z. Bao, Chem. Mater. **20**, 7332 (2008).